Hindawi
Complexity
Volume 2020, Article ID 8821050, 11 pages
https://doi.org/10.1155/2020/8821050

WILEY | Hindawi

Research Article

Fuzzy Logic Systems-Based Optimization and Control of Complicated High-Pressure Fuel Line with Double Fuel Injectors and One Pressure Reducing Valve

Dunqian Cao, Xue Zhang, Haoran Xue, and Conglin Xu

Guangxi University for Nationalities, Nanning 530006, China

Correspondence should be addressed to Dunqian Cao; caodunqian@gxun.edu.cn

Received 21 September 2020; Revised 16 October 2020; Accepted 24 October 2020; Published 5 November 2020

Academic Editor: Abdel-Haleem Abdel-Aty

High-pressure fuel line is a basic component of many modern industrial devices, and its pressure stability affects operating efficiency and safety. In this paper, the working mechanism of high-pressure fuel line with double fuel injectors and pressure reducing valve is studied as the main object, the differential equation for changes in pressure with time is established, and the rotating speed of high-pressure fuel pump cam, fuel injection time of fuel injector, and the threshold of pressure reducing valve are optimized using fuzzy logic systems to control the pressure in high-pressure fuel line within a safe range and improve the operating efficiency and safety of high-pressure fuel line. The results of numerical simulation show that the pressure reducing valve can effectively control the pressure in high-pressure fuel line.

1. Introduction

Fuel-powered engines play a very important role in production and daily life. The pressure in a high-pressure fuel line will change to a certain extent when fuel oil is introduced into and ejected from it, especially during intermittent operation, in which case the amount of fuel ejected will be different from the expected amount. Such deviation will affect the operating efficiency of fuel-powered engines and may even result in high-pressure fuel line rupture when the pressure reaches a certain level.

Figure 1 shows a high-pressure fuel line of certain model with an internal length of l and an inner diameter of d. Fuel (oil) is supplied by a high-pressure fuel pump to the high-pressure fuel line. A high-pressure fuel pump mainly consists of plunger housing, plunger, and cam. The cam rotates to drive the plunger to move reciprocally. When the plunger reaches the bottom dead center, the plunger housing will be filled with low-pressure fuel. When the plunger moves upwards to compress the fuel, the pressure in the plunger housing will increase gradually. When the pressure in the plunger housing exceeds that in the high-pressure fuel line, the check valve connecting the plunger housing and high-pressure fuel line will open to allow fuel oil to enter the high-pressure fuel line. When the plunger reaches the top dead center, it will start to move downwards and the pressure in the plunger housing will decline gradually. When the pressure in the plunger housing is lower than that in the high-pressure fuel line, the check valve will close. And when the plunger reaches the bottom dead center again, the plunger will be refilled with low-pressure fuel. This process is repeated, as shown in Figure 2. It is obvious that the inflow velocity is determined by the angular velocity of the rotating cam [1].

A high-pressure fuel line is usually fitted with one or two fuel injectors ejecting fuel oil at a fixed frequency. The amount of fuel ejected is related to various factors such as the pressure in high-pressure fuel line, the area of injector opening, and nozzle-opening time. High-pressure fuel injection systems are considered the most prospective fuel injection systems for direct injection diesel engines [2, 3]. In such systems, the pressure can be controlled flexibly and the amount of fuel injected is determined by system pressure and injection time. Therefore, the precision of pressure control is one of the important factors affecting the performance of fuel-powered engines [4].

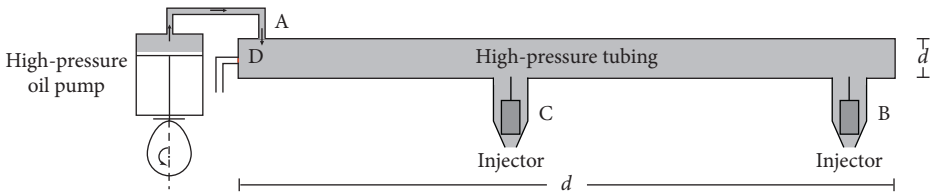

Figure 1: Schematic of the working mechanism of high-pressure fuel line.

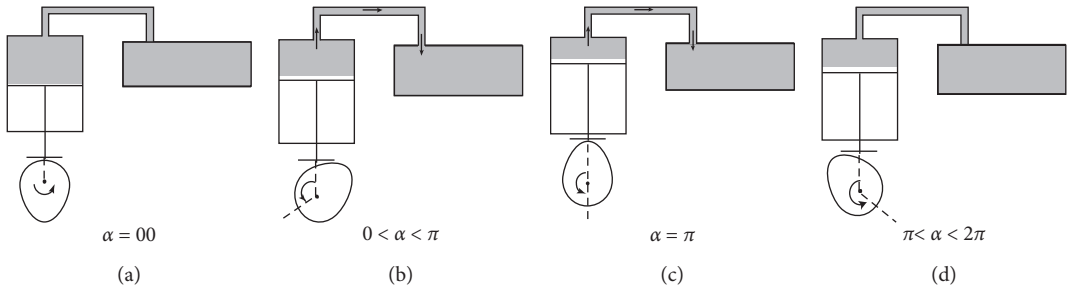

Figure 2: Schematic of the working mechanism of high-pressure fuel pump. (a) $\alpha = 0$. (b) $0 < \alpha < \pi$. (c) $\alpha = \pi$. (d) $\pi < \alpha < 2\pi$.

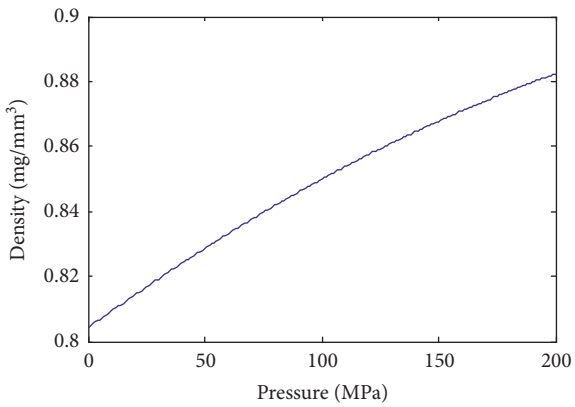

Figure 3: Relationship between the pressure and density of a certain fuel.

For fuel-powered engines operating under certain conditions, it is required that the pressure in high-pressure fuel line remain stable at a certain level and pressure surges be minimized, so that the amount of fuel injected can be controlled precisely [5, 6]. In [7], the multi-injection nozzle model was solved using the Monte Carlo method. This method is a random search algorithm, which is advantageous in that it does not require the first derivative of the objective function and is deficient in that it is highly random and unstable and converges slowly and that the solution found by it might be a local optimal solution. In [8], a difference equation-based model for determining cam angular velocity and a functional model-based check valve control scheme were established, and a scheme was developed for controlling cam angular velocity, injection rule, and pressure reducing valve parameters at constant pressure in several cases. In [9], a model for simulating and analyzing fuel injection systems with high-pressure fuel line was built using AVL-HYDSIM, and a series of parameters affecting the performance of such systems such as injection pressure were determined. In [10], a high-pressure fuel line pressure stabilization model based on first-order difference equation, a model for simulating pressure distribution in high-pressure fuel line, and a single-objective programming-based model for designing fuel injection systems were built using the ideas of the finite difference method, the method of characteristics, single-objective optimization, and exhaustive search, and different schemes were given for designing high-pressure fuel injection systems under different operating conditions of high-pressure fuel line. Additionally, this issue was also studied in [11, 12], in which the relationship between changes in pressure and cam angular velocity was given.

In [13], the rule of changes in pressure with the volume of high-pressure fuel line and the number of fuel injectors was determined through simulation and analysis. In [14], the rule of changes in average pressure surge with length-to-diameter ratio was determined through simulation and analysis. In [15], the relationship between changes in the amount of fuel injected by the system and pressure was identified through experiments. In [16], through experiments, an ideal filter was designed to eliminate vibration induced by water hammer pressure waves in high-pressure systems. Pressure surges have a significant impact on the performance of high-pressure systems, but there are few studies aimed at analyzing the rule of pressure surges in a segmented and detailed manner. Therefore, the rule of pressure surges needs to be further studied.

Excessively high internal pressure may cause instable operation and even rupture of a high-pressure fuel line. To avoid such phenomena, it is planned to install a pressure reducing check valve in the high-pressure fuel line to allow fuel oil to return to the external low-pressure fuel line when the internal pressure reaches a certain level, thus reducing the pressure in high-pressure fuel line.

The focus of this study is put on how to control the cam rotating speed, fuel injection time, and the threshold of pressure reducing valve, control the pressure in high-pressure fuel line within a certain stable range, and identify

the rule of changes in pressure with time. For simplicity, fuel density and pressure in the same chamber are assumed to be uniform at all times (Tables 1 and 2).

2. Preparations

2.1. Description of Symbols. Description of symbols is provided in Table 1.

2.2. Units. The units of the physical quantity are provided in Table 2.

2.3. Relationship between Fuel Pressure and Density. The relationship between fuel pressure P, density ρ, and elastic modulus E can be expressed as [17]

$$\frac{\mathbf{dP}}{\mathbf{d\rho}} = \frac{\mathbf{E}}{\boldsymbol{\rho}}. \tag{1}$$

If the relationship between the elastic modulus and density of a certain fuel complies with $E = aP^2 + bP + c$, the following formulas can be obtained by solving equation (1):

$$P = \Psi(\rho) = \frac{-b + W \cdot \tan(1/2 \cdot W \cdot \ln(\rho) + Z)}{2a}, \tag{2}$$

$$\rho = \Phi(P) = \exp\left(\frac{2}{W}\left(\arctan\left(\frac{2aP + b}{W}\right) - \pi - Z\right)\right), \tag{3}$$

where $W = \sqrt{4ac - b^2}$ and Z is an arbitrary constant. If fuel density is 0.85 when a known pressure of 100 is given,

$$Z = \arctan\left(\frac{(b + 200a)(1 + u_1u_2) - W(u_1 - u_2)}{W(1 + u_1u_2) + (b + 200a)(u_1 - u_2)}\right), \tag{4}$$

where $u_1 = \tan(1/2\ln(17)W)$, $u_2 = \tan(1/2\ln(20)W)$. Specifically, when

$$E = 0.02893P^2 + 3.077P + 1572, \tag{5}$$

then

$$P = \Psi(\rho) = 226.958\tan(6.566\ln(\rho) - 1.48) - 53.18, \quad 0.62 < \rho < 0.98, \tag{6}$$

$$\rho = \Phi(P) = 0.7765\exp(0.1523\arctan(0.0044P + 0.2343)), \quad P > 0. \tag{7}$$

Figure 3 shows the relationship between fuel pressure and density. The fuel mentioned in this paper refers to the fuel that complies with such relationship. The effect of temperature on the fuel is neglected.

2.4. Relationship of Fuel Flow Rate to Pressure and Density. The fuel flows from the high-pressure side to the low-pressure side through the small orifice. The amount of fuel flowing through the small orifice per unit time is

$$m = CA\sqrt{2\rho\Delta P}, \tag{8}$$

Table 1: Symbol description.

Symbol	Description
P	Pressure
ρ	Density
E	Elastic modulus
$\mathbf{m}$, $\mathbf{m}_i$	Fuel flow rate per unit time
$\mathbf{M}_i$	Fuel flow through the orifice
C	Flow coefficient of fuel
A	Area of small orifice
t	Time
γ	Polar radius of cam
α	Polar angle of cam
ρ_0	Fuel density in plunger housing
ρ_0	Density when plunger moves to bottom dead center
$\widehat{\rho}_0$	Density when plunger moves to top dead center
$\mathbf{V}_0$	Volume of plunger housing
$\mathbf{V}_0$	Volume when plunger moves to bottom dead center
$\widehat{V}_0$	Volume when plunger moves to top dead center
$\mathbf{d}_0$	Diameter of plunger housing
d_1	Diameter of small orifice at fuel inlet
A_1	Area of small orifice at fuel inlet
ω	Cam rotating speed
l	Length of high-pressure fuel line
d	Diameter of high-pressure fuel line
P_1	Internal combustion pressure in high-pressure fuel line
V_1	Volume of high-pressure fuel line
ρ_1	Fuel density in high-pressure fuel line
$\overline{P}$	Stable pressure in high-pressure fuel line
$\overline{M}_1$	Amount of oil into high-pressure fuel line per circle of cam rotation
d_2	Diameter of fuel injector needle valve
$\overline{d}_2$	Diameter of the lowest nozzle of fuel injector(s)
θ	Half-angle of fuel injector seal seat
h	Lift of needle valve
A_2	Area of fuel injector opening
d_4	Diameter of pressure reducing valve outlet
Ω	Threshold of pressure reducing valve

Table 2: Unit.

Physical quantity	Unit
Pressure	MPa
Density	mg/mm^3
Mass	mg
Time	ms
Angular velocity	rad/ms
Length	mm
Area	mm^2
Volume	mm^3

where C is the flow coefficient, A is the area of the small orifice, ΔP is the pressure difference between two sides of the small orifice, and ρ is fuel density on the high-pressure side. When the pressure on the low-pressure side is very small, m can be approximated to

$$m = CA\sqrt{2\rho P}. \tag{9}$$

2.5. Analysis of Fuel Pressure in Plunger Housing. Assuming that the cam shape is defined by polar angle and polar radius as $\gamma(\tau)$, $\gamma_{\min} = \gamma(\pi/2)$ and $\gamma_{\max} = \gamma(3\pi/2)$.

When the cam rotating angle is $\alpha = 0$, the plunger will move to the bottom dead center, the volume of plunger housing will reach its maximum, $\check{V}_0$, and the plunger housing will be filled with low-pressure fuel (with a density of $(\check{\rho}_0)$; when $\alpha = \pi$, the plunger will move to the top dead center and the volume of plunger housing will reach its minimum, $\hat{V}_0$. After the cam rotates α radians, the distance between the plunger and the top dead center is $\gamma_{\max} - \gamma(\alpha + \pi/2)$, and the volume of plunger housing will be

$$\begin{aligned} V_0(\alpha) &= \hat{V}_0 + \frac{\pi}{4} d_0^2 \cdot (h_\pi - h_\alpha) \\ &= \hat{V}_0 + \frac{\pi}{4} d_0^2 \cdot \left(\gamma_{\max} - \gamma\left(\alpha + \frac{\pi}{2}\right)\right), \end{aligned} \tag{10}$$

where d_0 is the diameter of plunger housing. It is obvious that

$$\check{V}_0 = V_0(0) = \hat{V}_0 + \frac{\pi}{4} d_0^2 \cdot (\gamma_{\max} - \gamma_{\min}), \tag{11}$$

and if the fuel does not enter the high-pressure fuel line, fuel density in the plunger housing will be

$$\rho_0(\alpha) = \frac{\check{\rho}_0 \check{V}_0}{V_0(\alpha)}, \tag{12}$$

and fuel pressure therein will be

$$P_0(\alpha) = \Psi(\rho_0(\alpha)). \tag{13}$$

If the fuel can enter the high-pressure fuel line and the pressure in high-pressure fuel line remains stable at $\overline{P}_1$, the amount of fuel into high-pressure fuel line per circle of cam rotation will be

$$\overline{M}_1 = \rho_0(0) V_0(0) - \Phi(\overline{P}_1) V_0(\alpha). \tag{14}$$

2.6. Area of Fuel Injector Opening. Assuming that the fuel injection nozzle has a structure shown in Figure 4, the diameter of needle valve is d_2, the seal seat is a cone with a half-angle of θ, and the diameter of the lowest nozzle is $\overline{d}_2$, when its lift is 0, the needle valve will close, when its lift is greater than 0, the needle valve will open, and the fuel will flow towards and be ejected through the injection nozzle.

Assuming that the relationship between the lift of needle valve and time within one fuel injection cycle is $h = h(t)$, then the area of fuel injector opening will be

$$A_2(t) = \begin{cases} \pi\left(\dfrac{d_2}{2} + h(t) \cdot \tan(\theta)\right)^2 - \dfrac{\pi}{4} d_2^2, & 0 \le h(t) \le \overline{h}, \\ \dfrac{\pi}{4} \overline{d}_2^2, & h(t) > \overline{h}, \end{cases} \tag{15}$$

where $\overline{h} = -d_2 + \sqrt{d_2^2 + \overline{d}_2^2}/2\tan(\theta)$. When the lift is relatively low, the area of fuel injector opening will be area of the clearance between the needle valve and the seal seat. When the lift is relatively high, the area of fuel injector opening will be area of the lowest injection nozzle of fuel injector(s).

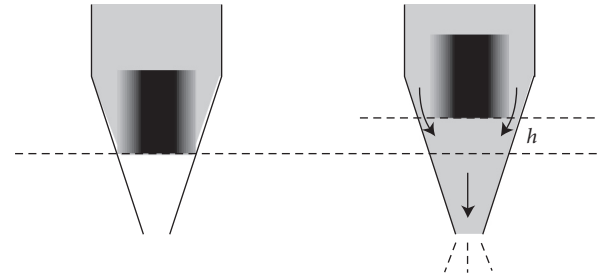

Figure 4: Working principle of fuel injector.

2.7. Working Principle of Pressure Reducing Valve. The pressure reducing check valve is connected to the high-pressure fuel line via a round pipe with a diameter of d_4. When the pressure in high-pressure fuel line is higher than Ω, the pressure reducing valve will open automatically to allow the fuel in high-pressure fuel line to flow back to the external low-pressure fuel line, thus reducing the fuel pressure in high-pressure fuel line. When the pressure in high-pressure fuel line is lower than Ω, the pressure reducing valve will close automatically. It can be easily known that the amount of fuel through the pressure reducing valve per unit time is

$$\begin{aligned} m_4(t) &= \begin{cases} C \cdot \dfrac{\pi}{4} d_4^2 \cdot \sqrt{2\rho_1(t) P_1(t)}, & P_1(t) > \Omega, \\ 0, & P_1(t) \le \Omega, \end{cases} \\ &= \operatorname{sign}(P_1(t) - \Omega) \cdot C \cdot \frac{\pi}{4} d_4^2 \cdot \sqrt{2\rho_1(t) P_1(t)}. \end{aligned} \tag{16}$$

3. Analysis of Fuel Density and Pressure in High-Pressure Fuel Line

Assuming that $P_0(t), P_1(t)$ are, respectively, fuel pressure in the plunger housing and that in the high-pressure fuel line at the time of t, $\rho_0(t), \rho_1(t)$ are, respectively, fuel density in the plunger housing and that in the high-pressure fuel line at the time of t, and V_1 is the volume of high-pressure fuel line, then $V_1 = ld^2/4\pi$. The amount of fuel from the high-pressure fuel pump into the high-pressure fuel line per unit time is $m_1(t)$, the amounts of fuel injected by two fuel injectors are $m_2(t - \mu_1)$ and $m_2(t - \mu_2)$, respectively, and the amount of fuel from the pressure reducing valve is $m_4(t)$. According to the law of conservation of mass, in a small time range of $[t, t + \Delta t]$,

$$\begin{aligned} (\rho_1(t + \Delta t) - \rho_1(t)) V_1 = (&m_1(t) - m_2(t - \mu_1) \\ &- m_2(t - \mu_2) - m_4(t)) \Delta t. \end{aligned} \tag{17}$$

Letting $\Delta t \longrightarrow 0$, by rearranging the formula above, the following equation can be obtained:

$$\frac{\mathrm{d}\rho_1(t)}{\mathrm{d}t} = \frac{1}{V_1}(m_1(t) - m_2(t - \mu_1) - m_2(t - \mu_2) - m_4(t)), \tag{18}$$

where

$$m_1(t) = \begin{cases} CA_1\sqrt{2\rho_0(t)\left(P_0(t) - P_1(t)\right)}, & P_0(t) > P_1(t), \\ 0, & P_0(t) < P_1(t), \end{cases}$$
$$= \operatorname{sign}\left(P_0(t) - P_1(t)\right) \cdot CA_1\sqrt{2\rho_0(t)\left(P_0(t) - P_1(t)\right)}, \tag{19}$$

$$m_2(t) = C \cdot A_2(t) \cdot \sqrt{2\rho_1(t)P_1(t)}, \tag{20}$$

$$m_4(t) = \begin{cases} C \cdot \frac{\pi}{4}d_4^2 \cdot \sqrt{2\rho_1(t)P_1(t)}, & P_1(t) > \Omega, \\ 0, & P_1(t) \le \Omega, \end{cases} \tag{21}$$
$$= \operatorname{sign}\left(P_1(t) - \Omega\right) \cdot C \cdot \frac{\pi}{4}d_4^2 \cdot \sqrt{2\rho_1(t)P_1(t)},$$

$$\operatorname{sign}(x) = \begin{cases} 0, & x \le 0, \\ 1, & x > 0. \end{cases} \tag{22}$$

These are the equations with which fuel density in the high-pressure fuel line complies. Fuel pressure can be calculated using formula (2). If the initial conditions are given, the numerical solutions to fuel density and pressure in the high-pressure fuel line can be found by difference method.

4. Fuzzy Logic Systems-Based Optimization and Control

Considering the changes in fuel pressure $P_1(t)$ in the high-pressure fuel line in a large time range of $[0, T_1]$, mean squared error is defined as follows to measure the degree of pressure deviation $\overline{P}$:

$$E = \frac{1}{T_1}\int_0^{T_1}\left(P_1(t) - \overline{P}\right)^2 \mathrm{d}t. \tag{23}$$

The objective of optimization is to find the solutions to cam rotating speed ω, fuel injection times 155 μ_1, μ_2, and pressure reducing valve threshold Ω and to minimize E. Therefore, the optimization 156 model can be expressed as

$$\min E\left(\omega, \mu_1, \mu_2, \Omega\right) = \frac{1}{T_1}\int_0^{T_1}\left(P_1(t) - \overline{P}\right)^2 \mathrm{d}t, \tag{24}$$

where $\omega > 0, \mu_1 \in [0, 2\pi/\omega], \mu_2 \in [\mu_1, 2\pi/\omega]$, $\Omega > \overline{P}_1$.

The optimization problem mentioned above can be solved in two cases: (1) when the high-pressure fuel line is not fitted with a pressure reducing valve and (2) when high-pressure fuel line is fitted with a pressure reducing valve.

4.1. High-Pressure Fuel Line without Pressure Reducing Valve. If the high-pressure fuel line is not fitted with a pressure reducing valve, $m_4(t) \equiv 0$ and problem (24) can be degenerated to

$$\min E\left(\omega, \mu_1, \mu_2\right). \tag{25}$$

To minimize $E(\omega, \mu_1, \mu_2)$, the amount of fuel into the high-pressure fuel line per unit time should be equal to the amount of fuel ejected per unit of time.

The amount of fuel that enters the high-pressure fuel line and the amount of fuel that is injected within a period of time should be equal. Based on the working cycle of the injector, the number of cam rotations is $\omega/2\pi T$ in one cycle, and one rotation enters the high pressure. The amount of fuel in the fuel pipe is $\overline{M}_1$. The amount of fuel injected by an injector in time T is $M_2(T)$. Since there are two injectors in this question, then we have

$$\frac{\omega}{2\pi}T \cdot \overline{M}_1 = 2M_2(T). \tag{26}$$

Then, the cam rotating speed should be

$$\omega = \frac{4\pi M_2(T)}{\overline{M}_1 \cdot T}, \tag{27}$$

where $M_2(T)$ is the amount of fuel ejected by a fuel injector in one operating cycle and $M_2(T) = \int_0^T m_2(t)\mathrm{d}t$.

Solving procedure is as follows:

(1) Estimate an initial rotating speed of $\omega^{(0)}$, and let $i = 0$, $\mu_1^{(0)} = \mu_2^{(0)} = T/2, \delta = 0.01, \varepsilon = 10^{-4}$.

(2) Let $\omega = \omega^{(i)}$, set search ranges $\mu_1 \in [0, T], \mu_2 \in [\mu_1, T]$, perform two-dimensional search for the solution to problem (25), and find the solutions to $\mu_1^{(i+1)}, \mu_2^{(i+1)}$.

(3) Let $\mu_1 = \mu_1^{(i+1)}, \mu_2 = \mu_2^{(i+1)}$, set search range $\omega \in [\omega^{(i)} - \delta, \omega^{(i)} + \delta s]$, perform one-dimensional search for the solution to ω, and find the solution to $\omega^{(i+1)}$.

(4) If $\delta < \varepsilon$, stop searching. Otherwise, reduce the search ranges for μ_1, μ_2, let $\delta = 0.5\delta$, $i = i+1$, and return to step (2).

4.2. High-Pressure Fuel Line with Pressure Reducing Valve. If the high-pressure fuel line is fitted with a pressure reducing valve, the operating cycle of the plunger housing may be assumed to be the same as that of fuel injector to stabilize the operation of high-pressure fuel line as far as practicable. In this case, $\omega = 2\pi/T$. Therefore, problem (24) can be degenerated to

$$\min E\left(\mu_1, \mu_2, \Omega\right). \tag{28}$$

The solving method for high-pressure fuel line with pressure reducing valve is similar to that for high-pressure fuel line without pressure reducing valve. The only difference is that, in the solving method for high-pressure fuel line with pressure reducing valve, the optimization of cam rotating speed ω is converted to that of pressure reducing valve threshold Ω and the initial Ω may be set to a value slightly higher than $\overline{P}_1$.

5. Numerical Simulation

Assuming that the length of high-pressure fuel line is $L = 500$ and the inner diameter thereof is $D = 10$, then the volume thereof is $V_1 = 12500\pi$. The initial fuel pressure in the high-

pressure fuel line is $P_1(0) = 100$ and fuel density therein is $\rho_1(0) = 0.85$. The diameter of the small orifice at fuel inlet is $d_1 = 1.4$. The shape of the cam is shown in Figure 5. The polar coordinate equation of its cam contour line is

$$\gamma(\tau) = \gamma_{\min} + \frac{\gamma_{\max} - \gamma_{\min}}{2}(1 - \sin(\tau)), \tag{29}$$

where $\gamma_{\min} = 2.414, \gamma_{\max} = 7.239$.

The inner diameter of plunger housing is $d_0 = 5$, and the volume of plunger housing when the plunger moves to the bottom dead center is $\widehat{V}_0 = 20$. The volume of plunger housing when the plunger moves to the top dead center is

$$\overset{\vee}{V}_0 = V_0(0) = \widehat{V}_0 + \frac{\pi}{4}d_0^2 \cdot (\gamma_{\max} - \gamma_{\min}) \approx 114.74. \tag{30}$$

The pressure of low-pressure fuel is $\overset{\vee}{\rho}_0 = 0.5$ and the density thereof is $\rho_0 = 0.8044$.

If the pressure in high-pressure fuel line remains constant at 100, the amount of fuel into the high-pressure fuel pump per circle of cam rotation will be

$$\overline{M}_1 = \overset{\vee}{\rho}_0 \overset{\vee}{V}_0 - \Phi(P_1)\widehat{V}_0 \approx \overset{\vee}{\rho}_0 \overset{\vee}{V}_0 - 100\widehat{V}_0 = 75.3041. \tag{31}$$

If there are no fuel injector and pressure reducing valve, the changes in the volume of plunger housing, fuel inflow, fuel pressure, and density in the high-pressure fuel line with time when the cam rotating speed is $\omega = 0.01$ are shown in Figures 6 and 7, respectively.

Figure 6 shows that when the plunger is rising and the pressure in the plunger cavity reaches a certain value, the fuel starts to enter the high-pressure fuel pipe and reaches a peak at a certain time. After that, the flow rate starts to decrease to 0.

Assuming that the diameter of fuel injector needle valve is $d_2 = 2.5$, the half-angle of seal seat is $\theta = \pi/20$, and the diameter of the lowest injection nozzle is $\overline{d}_2 = 1.4$, then the

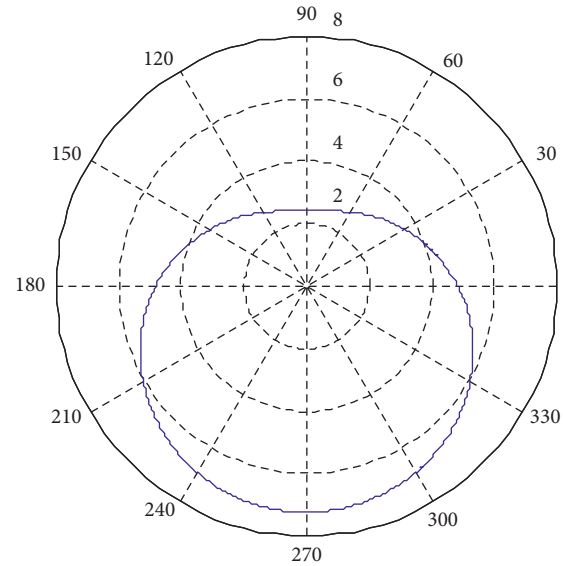

Figure 5: Shape of the cam.

relationship between the lift of needle valve and time within one injection cycle of $T = 100$ is

$$h(t) = \begin{cases} 1 - \cos\left(15.71\,t^2\right), & 0 \le t < 0.45, \\ 2, & 0.45 \le t \le 2, \\ 1 - \cos\left(15.71\,(t - 2.45)^2\right), & 2 < t < 2.45, \\ 0, & 2.46 \le t \le T, \end{cases} \tag{32}$$

According to formulas (15) and (32), the relationship between the area of fuel injector opening and time is as follows:

$$A_2(t) = \begin{cases} \pi\left(\frac{d_2}{2} + \left(1 - \cos\left(15.71\,t^2\right)\right) \cdot \tan(\theta)\right)^2 - \frac{\pi}{4}d_2^2, & 0 \le t \le 0.33, \\ \frac{\pi}{4}\overline{d}_2^2, & 0.33 < t < 2.12, \\ \pi\left(\frac{d_2}{2} + \left(1 - \cos\left(15.71\,(t - 2.45)^2\right)\right) \cdot \tan(\theta)\right)^2 - \frac{\pi}{4}d_2^2, & 2.12 \le t < 2.45, \\ 0, & 2.45 \le t \le T, \end{cases} \tag{33}$$

From formula (20), it can be known that the amount of fuel injected by a fuel injector in one injection cycle is

$$M_2(T) = C \cdot \sqrt{2\rho_1 P_1} \int_0^T A_2(t)\mathrm{d}t \approx 32.87890421. \tag{34}$$

To solve equation (18), time is evenly discretized into $t_0, t_1, t_2, \ldots, t_n, \ldots$, and the interval between two adjacent time points is set to Δt. If the volume of plunger housing $V_0(t_{i-1})$, fuel density in the plunger housing $\rho_0(t_{i-1})$, fuel pressure in the plunger housing $P_0(t_{i-1})$, fuel pressure in the high-pressure fuel line $P_1(t_{i-1})$, fuel density in the high-pressure fuel line $\rho_1(t_{i-1})$, fuel injector opening area $A_2(t_{i-1})$, injection times (at which the two fuel injectors start to operate) μ_1, μ_2, and pressure reducing valve threshold Ω at the time of t_{i-1} are known, fuel density in the high-pressure fuel line at the time of t_i will be

$$\begin{aligned} \rho_1(t_i) = \rho_1(t_{i-1}) + \frac{1}{V_1}\big(m_1(t_{i-1}) - m_2(t_{i-1} - \mu_1) \\ - m_2(t_{i-1} - \mu_2) - m_4(t_{i-1})\big)\Delta t, \end{aligned} \tag{35}$$

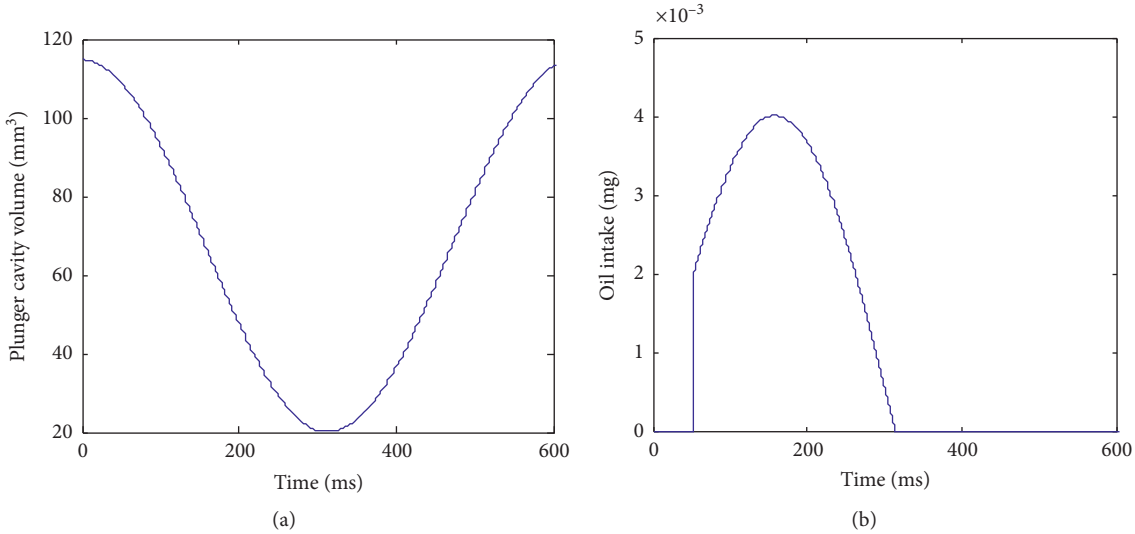

Figure 6: Changes in the volume of plunger housing and fuel inflow with time.

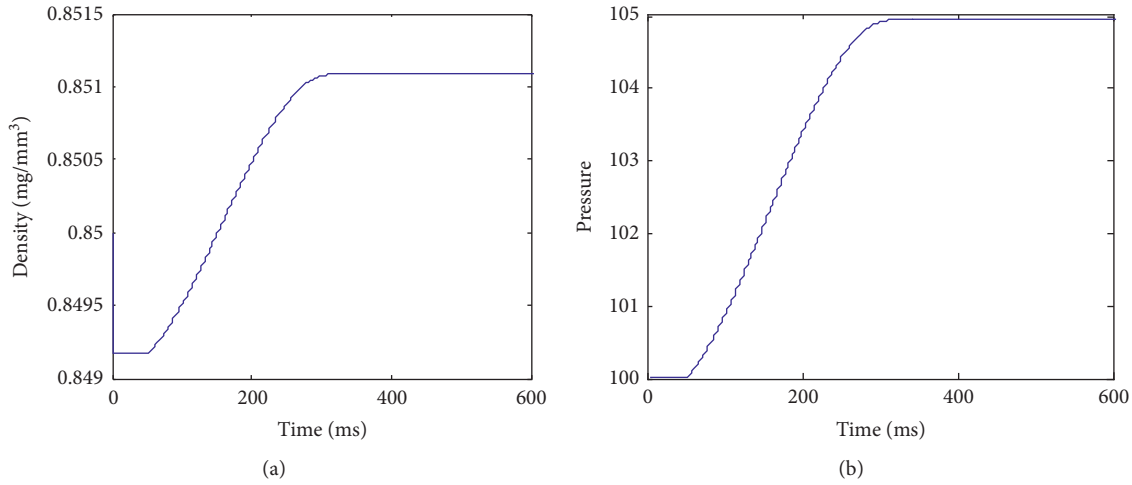

Figure 7: Changes in fuel pressure and density in the high-pressure fuel line with time.

where

$$
\begin{aligned}
m_1(t_{i-1}) &= \operatorname{sign}\left(P_0(t_{i-1}) - P_1(t_{i-1})\right)\cdot \mathrm{CA}_1\sqrt{2\rho_0(t_{i-1})\left(P_0(t_{i-1}) - P_1(t_{i-1})\right)},\\
m_2(t_{i-1}-\mu_1) &= C\cdot A_2(t_{i-1}-\mu_1)\cdot\sqrt{2\rho_1(t_{i-1})P_1(t_{i-1})},\\
m_2(t_{i-1}-\mu_2) &= C\cdot A_2(t_{i-1}-\mu_2)\cdot\sqrt{2\rho_1(t_{i-1})P_1(t_{i-1})},\\
m_4(t_{i-1}) &= \operatorname{sign}\left(P_1(t_{i-1}) - \Omega\right)\cdot C\cdot\frac{\pi}{4}d_4^2\cdot\sqrt{2\rho_1(t_{i-1})P_1(t_{i-1})}.
\end{aligned}
\tag{36}
$$

Fuel pressure can be calculated using formula (6) as follows: $P_1(t_i) = \Psi(\rho_1(t_i))$.

5.1. High-Pressure Fuel Line with Only One Fuel Injector. Assuming that the high-pressure fuel line is fitted with only one plunger house and one fuel injector, then $m_2(t-\mu_2) \equiv 0, m_4(t) \equiv 0$, $T_1 = 1000$, and the solutions found are as follows:

$$\begin{aligned} \omega &= 0.027186, \\ \mu_1 &= 0. \end{aligned} \tag{37}$$

In this case, the average fuel pressure in the high-pressure fuel line is $\overline{P}$ =99.946, the mean squared error is $E = 1.34898$, the minimum fuel pressure is $P_{\min} = 97.561$, and the maximum fuel pressure is $P_{\max}$ =102.552. The changes in fuel pressure are shown in Figure 8.

It can be seen from the simulation results that the pressure in the high-pressure fuel pipe is not completely cyclically changed, which will cause a slight difference in the amount of fuel injected by the injector every time in actual work, which may make the system work unstable.

5.2. High-Pressure Fuel Line with Two Fuel Injectors. Assuming that the high-pressure fuel line is fitted with two fuel injectors, then $m_4(t) \equiv 0$, and the solutions found are as follows:

$$\begin{aligned} \omega &= 0.054923, \\ \mu_1 &= 0, \\ \mu_2 &= 44. \end{aligned} \tag{38}$$

In this case, the average fuel pressure in the high-pressure fuel line is $\overline{P}$ =99.999, the mean squared error is $E = 1.231059$, the minimum fuel pressure is $P_{\min} = 97.574$, and the maximum fuel pressure is $P_{\max}$ =102.472. The changes in fuel pressure are shown in Figure 9.

Compared with the situation where there is only one injector, the two injectors make the average pressure in the high-pressure tubing closer to the target, and the variance is also improved, but the pressure is still not periodic.

5.3. High-Pressure Fuel Line with Two Fuel Injectors and One Pressure-Reducing Valve. When the high-pressure fuel line is fitted with two fuel injectors and one pressure reducing valve, the fuzzy system is used to optimize.

The fuzzy logic systems use IF-THEN rules to construct a mapping from an input vector $x(t) = [x_1(t), x_2(t), \ldots, x_n(t)]^T \in \mathcal{R}^n$ to an output $y(t) \in \mathcal{R}$. The r^{th} fuzzy rule can be written as

$$\mathcal{R}^r: \text{if } x_1(t) \text{ is } \mathrm{A}_1^r(x_1(t)) \text{ and } x_n(t) \text{ is } \mathrm{A}_n^r(x_n(t)) \text{ then } y(t) \text{ is } \mathrm{B}^r, \tag{39}$$

where A^r and B^r are fuzzy sets with membership functions $\mu_{\mathrm{A}_i^r}(x_i(t))$ and $\mu_{\mathrm{B}_i^r}(y(t))$, respectively. Suppose that $x(t)$ belongs to some compact set. By using the product-inference rule, singleton fuzzifier, and center-average defuzzifier, the output of fuzzy logic system can be expressed as [18,19]

$$y(t) = \frac{\sum_i^{n_r} \widetilde{y}^i(t)\left(\prod_{j=1}^n \mu_{A_j^i}(x_j(t))\right)}{\sum_{i=1}^{n_r}\left(\prod_{j=1}^n \mu_{A_j^i}(x_j(t))\right)} = \theta^T(t)\Psi(x(t)), \tag{40}$$

where n_r is the number of total fuzzy rules, $\widetilde{y}^i(t)$ is the point at which $\mu_{\mathrm{B}_i^r}(\widetilde{y}^i(t)) = 1$, $\mu_{\mathrm{A}_j^i}(x_j(t))$ is the membership function of the fuzzy variable $x_j(t)$ characterized by Gaussian, $\theta(t) = [\widetilde{y}^1(t), \widetilde{y}^2(t), \ldots, \widetilde{y}^{n_r}(t)]^{\mathrm{T}}$ is an adjustable parameter vector, and $\Psi = [\Psi^1, \Psi^2, \ldots, \Psi^{n_r}]^{\mathrm{T}}$ is a fuzzy basis vector, where Ψ^i is defined as

$$\Psi^i(x(t)) = \frac{\prod_{j=1}^n \mu_{A_j^i}(x_j(t))}{\sum_{i=1}^{n_r}\left(\prod_{j=1}^n \mu_{A_j^i}(x_j(t))\right).} \tag{41}$$

The structure of a fuzzy system is shown in Figure 10.where η, h, m are the numbers of neurons in the input, middle, and output layers, $w_k = [w_{k1}, \ldots, w_{kh}]^{\mathrm{T}}$, and $\varpi_k = [\varphi_{k1}\sum_{i=1}^n \nu_{1i}s_i + \theta_1, \ldots, \varphi_{kh}\sum_{i=1}^n \nu_{hi}s_i + \theta_h]^{\mathrm{T}}$. According

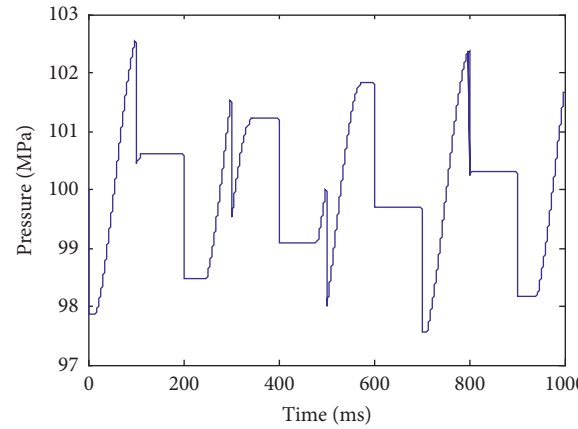

Figure 8: Changes in fuel pressure in high-pressure fuel line with only one fuel injector.

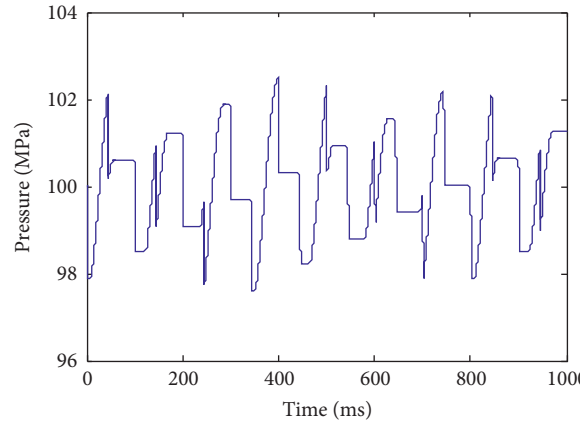

Figure 9: Changes in fuel pressure in high-pressure fuel line with two fuel injectors.

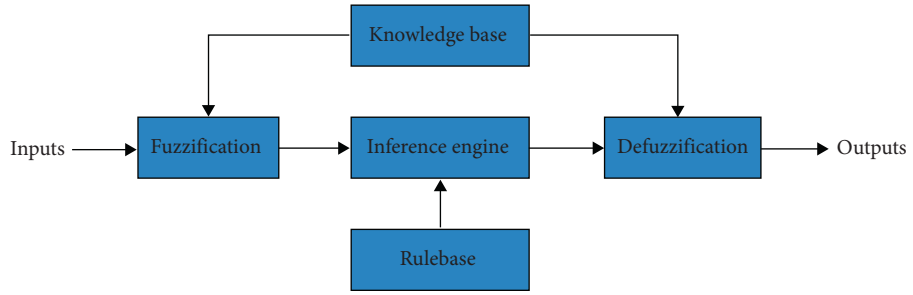

Figure 10: Structure of a fuzzy inference system. Its mathematical model can be expressed as [18–22]

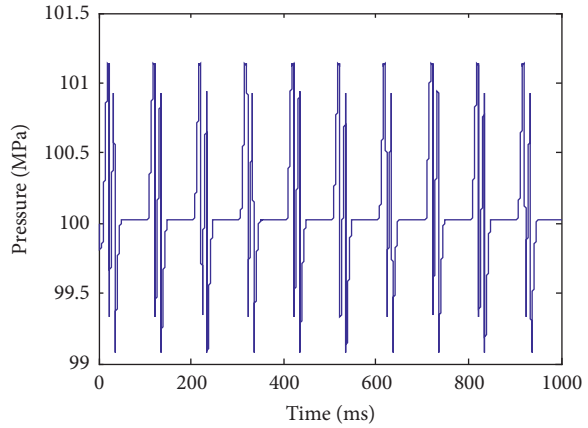

Figure 11: Changes in fuel pressure in high-pressure fuel line with two fuel injectors and one pressure reducing valve.

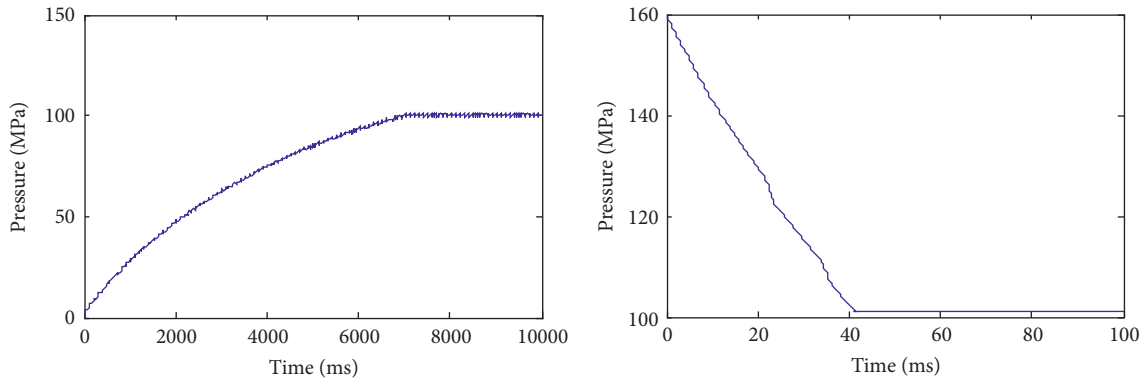

Figure 12: Schematic of fuel pressure recovery from low or high level to normal level.

to the universal approximation theorem, $\varphi(x) = e^x - e^{-x}/e^x + e^{-x}$ can be selected as function $\varphi(\cdot)$. Therefore, this system can be expressed as

$$y = \vartheta^T \psi(x), \tag{43}$$

where $\vartheta = [w_1^T, \ldots, w_m^T]^T$ and

$$\psi(\cdot) = \begin{bmatrix} \varpi_1(\cdot) & 0 & \cdots & 0 \\ 0 & \varpi_2(\cdot) & \cdots & 0 \\ \vdots & \vdots & \ddots & \vdots \\ 0 & 0 & \cdots & \varpi_m(\cdot) \end{bmatrix}.$$

$$y_k(s, w_k) = \sum_{j=1}^{h} w_{kj} \varphi_{kj} \left(\sum_{i=1}^{\eta} v_{ji} s_i + \theta_j \right) = w_k^T \varpi_k(\cdot), \tag{42}$$

The optimization is achieved using the fuzzy logic systems above and the solutions found are as follows:

$$\begin{aligned} \mu_1 &= 21.4, \\ \mu_2 &= 33.7, \\ \Omega &= 101.14. \end{aligned} \tag{44}$$

The average fuel pressure is $\overline{P}$ =100.092, the minimum fuel pressure is $P_{\min}$ =99.078, the maximum fuel pressure is $P_{\max}$ =101.145, and the mean squared error is $E = 0.151434$. The changes in fuel pressure are shown in Figure 11.

From the simulation results, the pressure shows a periodic change, and the fluctuation range is very small. The results of numerical simulation show that the pressure reducing valve plays a significant role in stabilizing fuel pressure (the mean squared error for high-pressure fuel line fitted with a pressure reducing valve is only 12.3% of that for high-pressure fuel line without pressure reducing valve).

The system can automatically restore the normal pressure level even if fuel pressure rises or drops abruptly due to certain reasons. The process of pressure recovery from 0.5 MPa to 100 MPa takes 6917.7 ms approximately and the process of pressure recovery from 160 MPa to 100 MPa only needs 42.41 ms (Figure 12).

6. Conclusion

In this study, a differential equation-based model for simulating the changes in fuel density with time is built based on the analysis of changes in fuel density and pressure in the high-pressure fuel line. The calculation results show that when no pressure reducing valve is provided, the effect of double fuel injectors is equivalent to that of a single fuel injector. The only difference is that the fuel inflow and the amount of fuel injected by double fuel injectors are two times those by a single fuel injector, and there is no significant difference in pressure changes in the high-pressure fuel line. If a pressure reducing valve is provided, the operating cycle of the high-pressure fuel pump may be set to the same period as that of fuel injector(s), and the system is still able to maintain fuel pressure at a normal level. By adjusting the fuel injection time of fuel injector(s) and the threshold of pressure reducing valve, fuel pressure in the high-pressure fuel line can be controlled within a small range of fluctuations, the amount of fuel injected in each injection cycle can be maintained at almost the same level, and the operating efficiency and stability of fuel-powered engines can be improved significantly.

Data Availability

The data used to support the findings of this study are included within the article.

Conflicts of Interest

The authors declare that there are no conflicts of interest regarding the publication of this paper.

References

[1] P. N. Brittain and J. D. Kirkpatrick, "Process for lining high pressure pipeline," US Patent 4496499, 1985.

[2] B. Mohan, W. Yang, K. L. Tay, and W. Yu, "Experimental study of spray characteristics of biodiesel derived from waste cooking oil," *Energy Conversion and Management*, vol. 88, pp. 622–632, 2014.

[3] P. Lucio, B. Giacomo, C. P. Francesco et al., "Zeuch method-based injection rate analysis of a common-rail system operated with advanced injection strategies," *Fuel*, vol. 128, pp. 188–198, 2014.

[4] H. Akiyama, H. Yuasa, A. Kato et al., "Precise fuel control of diesel common-rail system by using OFEM," *SAE International*10 pages, 2010.

[5] B. Meng, C. Gu, L. Zhang et al., "Hydrogen effects on X80 pipeline steel in high-pressure natural gas/hydrogen mixtures," *International Journal of Hydrogen Energy*, vol. 42, no. 11, pp. 7404–7412, 2017.

[6] X. Liu, A. Godbole, C. Lu, G. Michal, and V. Linton, "Investigation of the consequence of high-pressure CO_2 pipeline failure through experimental and numerical studies," *Applied Energy*, vol. 250, pp. 32–47, 2019.

[7] M. H. Abbas, R. Norman, and A. Charles, "Neural network modelling of high pressure CO_2 corrosion in pipeline steels," *Process Safety and Environmental Protection*, vol. 119, pp. 36–45, 2018.

[8] K. Shibanuma, T. Hosoe, H. Yamaguchi, M. Tsukamoto, K. Suzuki, and S. Aihara, "Crack tip opening angle during unstable ductile crack propagation of a high-pressure gas pipeline," *Engineering Fracture Mechanics*, vol. 204, pp. 434–453, 2018.

[9] F. Gao, C. Ji, Y. Yu et al., "Numerical simulation on fracture mechanics behavior of high-pressure gas pipeline," *Vibroengineering PROCEDIA*, vol. 21, pp. 208–213, 2018.

[10] J. Kec and I. Cerny, "Stress-strain assessment of dents in wall of high pressure gas pipeline," *Procedia Structural Integrity*, vol. 5, pp. 340–346, 2017.

[11] O. Adibi, N. Najafpour, B. Farhanieh et al., "Determination of safety distance around gas pipelines using numerical methods," *International Journal of Mechanical and Mechatronics Engineering*, vol. 12, no. 2, pp. 120–124, 2018.

[12] L. Qian, "Study on calculation and arrangement of high temperature and high pressure gas Pipeline," *Chemical Engineering Design Communications*, vol. 12, p. 110, 2017.

[13] S. R. Ravula, S. C. Narasimman, L. Wang, and A. Ukil, "Experimental validation of leak and water-ingression detection in low-pressure gas pipeline using pressure and flow measurements," *IEEE Sensors Journal*, vol. 17, no. 20, pp. 6734–6742, 2017.

[14] Y. Deng, H. Hu, B. Yu, D. Sun, L. Hou, and Y. Liang, "A method for simulating the release of natural gas from the rupture of high-pressure pipelines in any terrain," *Journal of Hazardous Materials*, vol. 342, pp. 418–428, 2018.

[15] D. Houssin-Agbomson, G. Blanchetière, D. McCollum et al., "Consequences of a 12 mm diameter high pressure gas release on a buried pipeline. Experimental setup and results," *Journal of Loss Prevention in the Process Industries*, vol. 54, pp. 183–189, 2018.

[16] L. Cheng, C. Ji, M. Zhong, Y. Long, and F. Gao, "Full-scale experimental investigation on the shock-wave characteristics of high-pressure natural gas pipeline physical explosions," *International Journal of Hydrogen Energy*, vol. 44, no. 36, pp. 20587–20597, 2019.

[17] M. Bogucki and M. Polonski, "Risk analysis for high pressure gas pipeline construction schedule," in *Proceedings of IOP Conference Series: Materials Science and Engineering*, vol. 471, February 2019, Article ID 112042.

[18] H. Liu, S. Li, H. Wang, and Y. Sun, "Adaptive fuzzy control for a class of unknown fractional-order neural networks subject to input nonlinearities and dead-zones," *Information Sciences*, vol. 454-455, pp. 30–45, 2018.

[19] Y. Zhou, H. Liu, J. Cao, and S. Li, "Composite learning fuzzy synchronization for incommensurate fractional-order chaotic systems with time-varying delays," *International Journal of Adaptive Control and Signal Processing*, vol. 33, no. 12, pp. 1739–1758, 2019.

[20] H. Liu, Y. Pan, C. Jinde, W. Hongxing, and Z. Yan, "Adaptive neural network backstepping control of fractional-order nonlinear systems with actuator faults," *IEEE Transactions on Neural Networks and Learning Systems*, 2020.

[21] H. Liu, H. Wang, J. Cao, A. Alsaedi, and T. Hayat, "Composite learning adaptive sliding mode control of fractional-order nonlinear systems with actuator faults," *Journal of the Franklin Institute*, vol. 356, no. 16, pp. 9580–9599, 2019.

[22] Y. Zhou, H. Wang, and H. Liu, "Generalized function projective synchronization of incommensurate fractional-order chaotic systems with inputs saturation," *International Journal of Fuzzy Systems*, vol. 21, no. 3, pp. 823–836, 2019.